Available online at www.sciencedirect.com

SCIENCE DIRECT®

Infrared Physics & Technology 48 (2006) 154–162

INFRARED PHYSICS & TECHNOLOGY

www.elsevier.com/locate/infrared

Wavelength modulation photoacoustic spectroscopy: Theoretical description and experimental results

Stéphane Schilt *, Luc Thévenaz

Ecole Polytechnique Fédérale de Lausanne (EPFL), Nanophotonics and Metrology Laboratory (NAM), CH-1015 Lausanne, Switzerland

Received 18 April 2005
Available online 2 November 2005

Abstract

A theoretical description of photoacoustic spectroscopy generated by wavelength modulation of a semiconductor laser source is reported for a Lorentzian absorption line. This model describes the first- and second-harmonic photoacoustic signals produced by a current-modulated semiconductor laser. Combined intensity- and wavelength-modulation is considered with arbitrary phase shift. Experimental results obtained when probing a CO_2 absorption line with a 2-μm distributed feedback laser are presented and validate the relevance of the reported model.

PACS: 42.55.Px; 42.60.Fc; 42.62.Fi

Keywords: Wavelength modulation; Photoacoustic spectroscopy; Trace gas monitoring; DFB lasers

1. Introduction

Infrared tunable lasers constitute ideal light sources for trace gas spectroscopy due to their unique combination of excellent spectroscopic and technical properties, such as narrow linewidth, tunability, compactness, long lifetime or room-temperature operation. They are composed of near-infrared (NIR) InGaAsP-based semiconductor laser diodes initially developed for the optical telecommunication market ($\lambda < 2$ μm), antimonide-based laser diodes in the 2–3 μm range and quantum cascade lasers (QCL) in the mid-infrared ($\lambda > 4$ μm). All these types of infrared lasers may be fabricated with a distributed feedback (DFB) structure, enabling to get singlemode emission, continuously tunable over several wavenumbers. Narrow-linewidth and broadly tunable external cavity diode laser (ECDL) in the NIR wavelength range are other suitable sources for high-resolution gas spectroscopy, whereas the gap in primary laser sources in the 3–4 μm range may be overcome by generating optical radiation by non-linear methods, such as difference frequency generation (DFG), optical parametric oscillation (OPO) or optical parametric generation/amplification (OPG/OPA).

* Corresponding author. Tel.: +41 21 693 3969; fax: +41 21 693 2614.
E-mail addresses: stephane.schilt@epfl.ch (S. Schilt), luc.thevenaz@epfl.ch (L. Thévenaz).

1350-4495/$ - see front matter
doi:10.1016/j.infrared.2005.09.001

Singlemode emission is essential to achieve high selectivity in gas sensing. Tunability enables precise adjustment of the laser emission on an absorption line of the target species, which is necessary for high sensitivity detection. Semiconductor lasers can also be easily and rapidly modulated, through a modulation of their injection current. Laser modulation capability is a key issue for high sensitivity gas detection and many of the most performant techniques for trace gas monitoring make use of laser modulation for efficient noise reduction and high sensitivity detection. This is for example the case in wavelength modulation spectroscopy (WMS) [1], frequency modulation spectroscopy (FMS) [2] and two-tone FMS [3], which use different modulation/demodulation schemes in order to reject the large offset in the DC-coupled optical transmission signal, or photoacoustic (PA) spectroscopy (PAS) [4–16], which measures the optical energy absorbed in the sample.

In a semiconductor laser, modulation of the injection current results in simultaneous modulation of the optical power (intensity modulation—IM) and of the laser frequency (wavelength or frequency modulation—WM/FM[1]). WMS/FMS techniques take advantage of the WM/FM properties of the laser in order to generate an offset-free derivative signal of the sample transmission. In that case, IM generally acts as a residual undesirable effect that distorts the signals. The situation is radically different for PAS. This technique is also based on the absorption of a modulated laser radiation by the molecules of the target species, but it directly responds to the energy absorbed in the sample and not to the transmitted energy. Therefore, it is intrinsically a zero-background technique. The absorbed optical energy is measured through an acoustic wave induced by periodic thermal expansion of the sample, resulting from periodic light absorption. This may be produced either through IM or WM of the laser radiation. The amplitude of this acoustic wave, measured using a sensitive miniature microphone, is directly proportional to the gas concentration. As PA signal is also directly proportional to the laser power, this technique has been primarily implemented using high power mid-infrared gas lasers (mainly CO_2 lasers), in order to achieve extreme detection limits in the ppb range [4–6]. In that case, IM has been naturally used, either using an external modulation (mechanical chopper), or with direct modulation of a RF-excited CO_2 laser. The theoretical description of the generation and detection of the PA signal, which has been given in detail by several authors [7–9], is well adapted to this situation, as it usually considers IM as an excitation source for the generation of the PA signal.

However, application of PAS using semiconductor lasers has increased in the recent years for three main reasons: (i) the improvement of the emission power of telecom-type NIR DFB lasers, which can deliver up to several tens of mW; (ii) the availability of NIR fibre amplifiers, capable of amplifying laser radiation by 20–30 dB, thus achieving amplified power in the range of 1 W and therefore improving the PAS sensitivity by 2–3 orders of magnitude [10,11]; (iii) the improvement of the characteristics of QCL in the MIR range, which have also demonstrated to be suitable light sources for PAS [12–14]. Similarly to gas lasers, semiconductor lasers may be intensity-modulated to generate a PA signal. This may be accomplished either using a mechanical chopper or, more generally, by directly switching on and off the laser injection current. But these lasers also offer the possibility to be wavelength-modulated, by modulating their injection current with a reduced amplitude in order to tune the laser on-line and off-line. Such a modulation scheme may give some advantages in certain conditions. For example, window noise and wall noise are efficiently suppressed for WM and harmonic detection [15]. WM may also be slightly more efficient than IM in the generation of the PA signal [16]. The theory of WMS (in the standard case of optical detection) is well documented in the literature. The first models, presented by Arndt [17], Reid and Labrie [18], or Supplee et al. [19], only treated the case of pure WM. Later, more complete models taking into account simultaneous WM and IM were presented by Philippe and Hanson [20], then Kluczynski et al. In a series of papers [21–24], these authors developed a complete theory of WMS based on Fourier decomposition. More recently, we also developed an analytical expression of WMS harmonic signals in the particular case of a Lorentzian lineshape, but for the general situation of combined IM–FM with arbitrary phase shift [25].

[1] A distinction is usually made in the literature between WM and FM: WM is generally used when the laser modulation frequency is much smaller than the absorption linewidth, whereas FM is used when the modulation frequency is larger than the absorption linewidth. However, these denominations may produce some confusion, as a current modulation always induces a modulation of both the laser wavelength and frequency. In this paper, we independently use these two denominations to represent the same effect.

PAS in combination with WM has already been discussed in the literature [10,26–30], but mainly in the experimental point of view and explicit mathematical theory of WM-induced PAS (WM-PAS) has not been given. Even if this situation presents some similarities with standard WMS, there is however an important distinction due to the fundamental difference in the techniques, i.e. WMS responds to the light transmitted through the analyzed sample, whereas PAS is sensitive to the absorbed energy. A general theory of WM-PAS is necessary in order to have a better understanding of this technique and to enable precise optimization of the modulation parameters. We report here a theoretical analytical description of WM-PAS that also takes into account the laser residual amplitude modulation arising when modulating the injection current in a semiconductor laser. Our description is based on the analytical model of WMS we previously developed in the case of a Lorentzian absorption line [25]. This model was a generalization of Arndt's theory [17], extended to the general case of simultaneous IM–FM with arbitrary phase shift.

Although the analytical WM-PAS model presented here applies to Lorentzian lineshapes only, it remains quite general, as most of the application of PAS concern gas monitoring in standard environmental conditions, i.e., at ambient temperature and atmospheric pressure. In such conditions, the general Voigt lineshape is properly approximated by a Lorentzian profile and our model thus properly applies to the case of PA trace gas detection at atmospheric pressure. The results of this theoretical model are compared with experimental measurements performed when a CO_2 absorption line is probed by a DFB laser emitting in the 2-μm wavelength range.

2. Theoretical description of PAS in presence of simultaneous IM–FM

Our theoretical description of WM-PAS is based on the analytical formalism developed in the case of WMS, when a Lorentzian absorption line is scanned by a laser diode with combined IM–FM with arbitrary phase shift Ψ [25]. In WM-PAS, the frequency of the detected PA signal needs to correspond to a resonance frequency f_{res} of the PA cell. Therefore, the laser is modulated at frequency $f_{\text{mod}} = f_{\text{res}}/n$ when the nth harmonic signal is considered. In addition to this modulation (generally performed in the kHz range), the laser wavelength is scanned through the absorption line using a slow current ramp at frequency F.

Using the same terminology as in our WMS model, the laser WM is described by the normalized frequency

$$x = x_0 - m\cos(2\pi f_{\text{mod}} t), \tag{1}$$

where $x = (\nu - \nu_{\text{line}})/\Delta\nu_{\text{line}}$ is the optical frequency ν normalized to the line parameters, ν_{line} the absorption line centre and $\Delta\nu_{\text{line}}$ the linewidth (half width at half maximum, HWHM). WM amplitude is characterized by the FM index $m = \Delta\nu/\Delta\nu_{\text{line}}$, which represents the maximum laser frequency deviation $\Delta\nu$ normalized by the absorption linewidth $\Delta\nu_{\text{line}}$.

Laser IM is taken into account by introducing a linear variation with slope p in the incident optical power as a function of the frequency

$$I_0(x) = I_0(p\Delta\nu_{\text{line}}x + 1). \tag{2}$$

In this expression, I_0 is the optical power at line centre, whereas slope p describes the laser power variation as a function of the optical frequency (in $[1/\text{cm}^{-1}]$). The light absorbed in the cell is given, in the case of a weakly absorbing sample, by

$$I_{\text{abs}}(x) = I_0(x)a(x) = I_0[p\Delta\nu_{\text{line}}x + 1]a(x), \tag{3}$$

where $a(x)$ is the absorbance of the sample. For Lorentzian lineshape,

$$a(x) = a_0\frac{1}{1+x^2}, \tag{4}$$

where a_0 is the absorbance at line centre.

Since WM efficiency of a semiconductor laser depends on modulation frequency, the p coefficient takes a different value for either the sine modulation at angular frequency $\omega = 2\pi f_{\text{mod}}$ or for the low frequency ramp used to scan the laser line through the absorption feature. Two different coefficients p_ω and p_Ω are therefore introduced to describe the laser optical power variation [25]. The first one is associated to the modulation frequency ω and the second to the low frequency ramp at $\Omega = 2\pi F$.

The determination of the PA signal generated at the two first harmonics ($1f$ and $2f$ signals) follows a similar procedure to the case of WMS, the only difference being that we consider the energy absorbed in the sample instead of the transmitted energy. The in-phase (p) and quadrature (q) PA signals at frequency $1f$ and $2f$ are respectively given by

$$\begin{cases} s_{PA,1p}(x) = -s_{1p}(x) - p_\omega\Delta\nu_{\text{line}}m, \\ s_{PA,1q}(x) = -s_{1q}(x), \end{cases} \tag{5a}$$

$$\begin{cases} s_{PA,2p}(x) = -s_{2p}(x), \\ s_{PA,2q}(x) = -s_{2q}(x), \end{cases} \quad (5b)$$

where functions $s_{1p}(x)$, $s_{1q}(x)$, $s_{2p}(x)$ and $s_{2q}(x)$ correspond to in-phase and quadrature signals in the case of standard WMS [25]. PA signals obtained for arbitrary detection phase Φ_n are given by

$$\begin{cases} s_{PA,1\Phi_1}(x) = s_{PA,1p}(x)\cos\Phi_1 + s_{PA,1q(x)}\sin\Phi_1, \\ s_{PA,2\Phi_2}(x) = s_{PA,2p}(x)\cos\Phi_2 + s_{PA,2q}(x)\sin\Phi_2. \end{cases} \quad (6)$$

PA signals of maximum and minimum amplitude are respectively reached for detection phases $\Phi_{n,\max}$ and $\Phi_{n,\min}$:

$$\Phi_{n,\max} = n\Psi + k\pi, \quad (7a)$$

$$\Phi_{n,\min} = n\Psi + (2k+1)\pi/2. \quad (7b)$$

Harmonic PA signals generated for combined IM–FM correspond, except for the sign, to WMS signals. This is quite intuitive as PAS measures the energy absorbed in the sample (I_{abs}), whereas WMS detects the transmitted energy ($I_{\text{trans}} = I_0 - I_{\text{abs}}$). Additional difference also occurs in the in-phase signal at frequency f ($s_{PA,1p}$), for which the background level is zero, whereas an offset appears in the standard WMS case, due to laser residual IM. The background level of WM-PAS signal is zero at each harmonic, as PAS is a zero-background technique.

3. Experimental results

PAS has been implemented using a DFB laser with emission wavelength corresponding to the R16 line in the $\nu_1 + 2\nu_2 + \nu_3$ band of CO_2 around 4990 cm^{-1}. Measurements have been performed at local atmospheric pressure, where the absorption line is well approximated by a Lorentzian lineshape function, as shown in Fig. 1. Table 1 lists the line parameters experimentally measured and compares them to the values obtained from HITRAN database [31]. A scheme of the experimental set-up is shown in Fig. 2. The laser is temperature-stabilized

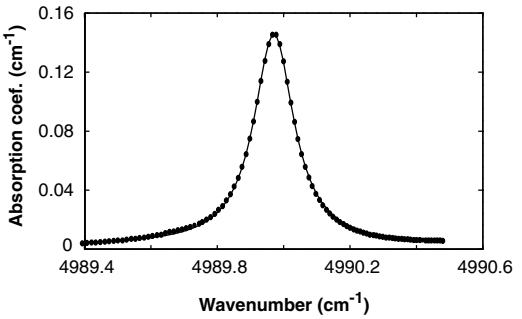

Fig. 1. R16 absorption line of CO_2 measured by optical transmission using a DFB laser emitting at 4990 cm^{-1}. The laser frequency was measured using a wavemeter with a resolution of 1 pm. Circle are experimental points and the line results from a fit by a Lorentzian distribution.

Table 1
Parameters of R16 CO_2 absorption line in the $\nu_1 + 2\nu_2 + \nu_3$ band. Comparison between experimental measurements and HITRAN database values

Line parameter	Symbol	Exp. value	HITRAN value	Unit
Central frequency	ν_{line}	4989.971 ± 0.003	4989.973	[cm^{-1}]
Linewidth	$\Delta\nu_{\text{line}}$	0.0732 ± 0.0007	0.07327	[cm^{-1}]
Line intensity	S	$(1.34 \pm 0.04) \times 10^{-21}$	1.328×10^{-21}	[cm^{-1}/(mol cm^{-2})]

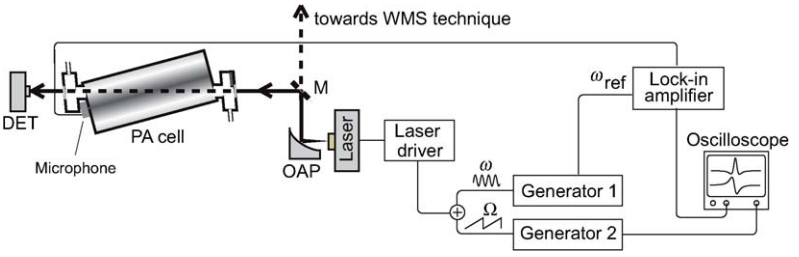

Fig. 2. Scheme of the experimental set-up used to implement the WM-PAS technique. OAP: off-axis parabolic mirror, DET: detector. A mobile mirror (M) enables to easily switch between PAS and WMS.

and driven by a commercial laser current supply. The laser beam is collimated using an off-axis-parabolic mirror (OAP) and is launched into a PA cell operated in its first radial mode around 10.5 kHz. The acoustic resonance is narrow (14 Hz HWHM), which corresponds to a quality factor $Q \cong 680$, as shown in Fig. 3. The small width of this resonance requires precise adjustment of the laser modulation frequency. The acoustic signal is detected using an electret microphone (Sennheiser KE 13-227) and is measured using a lock-in amplifier. The PA signal is normalized by the laser power, measured at the PA cell exit using a thermal powermeter.

Two different types of laser modulation have been considered for the generation of the PA signal. Firstly, IM has been applied, since this type of modulation is the most frequently used in PAS. IM has been obtained by modulating on and off the laser injection current with a square waveform (from threshold up to the current limit). In that case, pure IM is not exactly achieved, as residual WM also occurs. However, IM is largely dominant in this situation (the IM index M is unitary, $M = 1$) and it may be considered that IM is essentially obtained in this case. The other type of modulation that was considered is WM. To achieve WM, the laser current was modulated with a sine waveform of reduced amplitude (incomplete modulation in order to have small residual IM). Even if pure WM is not achieved in this case, this modulation is strongly dominant with respect to residual IM. A comparison of the CO_2 PA spectrum measured in the 4990 cm^{-1} range for the two types of modulation is shown in Fig. 4. As expected, CO_2 absorption spectrum is directly observed when IM is considered, whereas a derivative of the spectrum is obtained with WM.

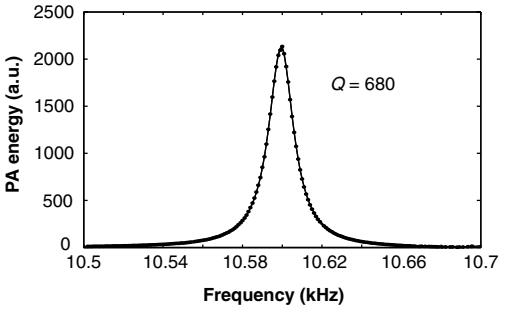

Fig. 3. Frequency distribution of the acoustic energy in the first radial mode of the PA cell. Circles are experimental points and the curve is the result of a fit by a Lorentzian distribution. The quality factor is $Q = 680$.

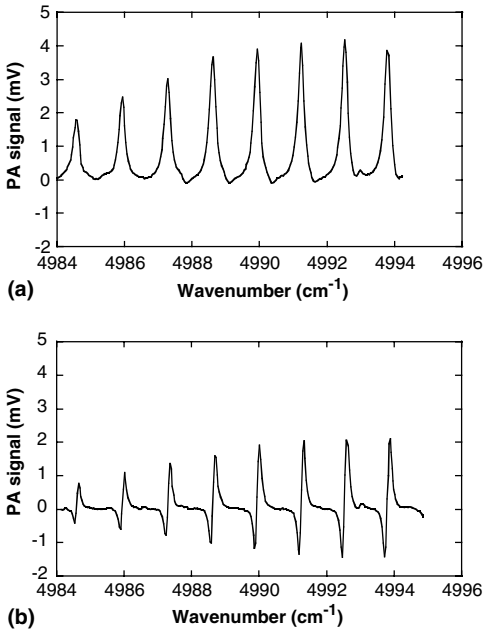

Fig. 4. CO_2 PA spectrum obtained for two different modulation schemes of the laser: (a) IM (on–off modulation of the laser current); (b) WM (sine modulation of the laser current with reduced amplitude).

Direct observation of WM-induced harmonic PA signal on an oscilloscope (as usually made in standard WMS) requires that the laser modulation frequency is adjusted to $f_{mod} = f_{res}/n$ when the nth harmonic signal is considered. In addition, the frequency F of the slow current scan used to sweep the laser through the analyzed absorption line must be much smaller than the width (HWHM) of the acoustic resonance ($F \ll \Delta f$), in order that the effective detection frequency ($f_{eff} = nf_{mod} \pm kF$, where k describes the principal Fourier components of the current ramp) lies within the acoustic resonance. For our narrow radial resonance, a current ramp at $F = 0.95$ Hz was experimentally used for the

Table 2
Summary of the different frequencies used for laser modulation and acoustic detection in the case of 1f and 2f WM-PAS signals

Parameter	Harmonic signals	
	$n = 1$	$n = 2$
Slow sweep frequency (F)	0.95 Hz	
Laser sine modulation frequency (f_{mod})	10.5 kHz	5.75 kHz
Acoustic detection frequency (f_{res})	10.5 kHz	
Acoustic resonance width (Δf)	14 Hz	

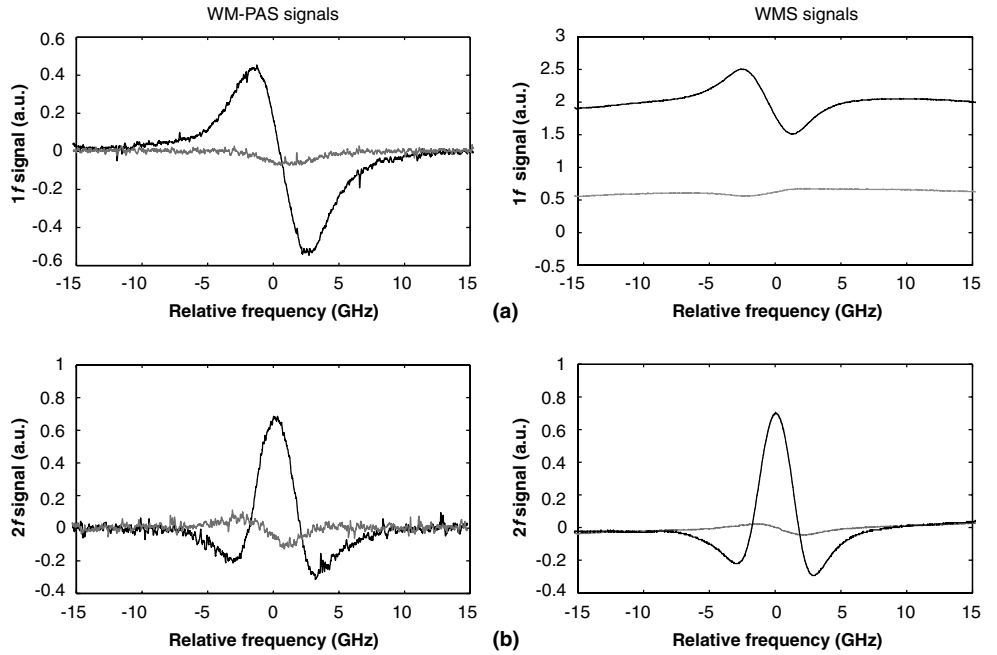

Fig. 5. Comparison of $1f$ (a) and $2f$ (b) signals obtained by WM-PAS and WMS for the same modulation conditions ($m = 1$). In each case, the phase of the lock-in detection has been adjusted in order to obtain the signal of maximum (black curves, $\Phi_n = \Phi_{n,\max}$) and minimum amplitude (grey curves, $\Phi_n = \Phi_{n,\min}$).

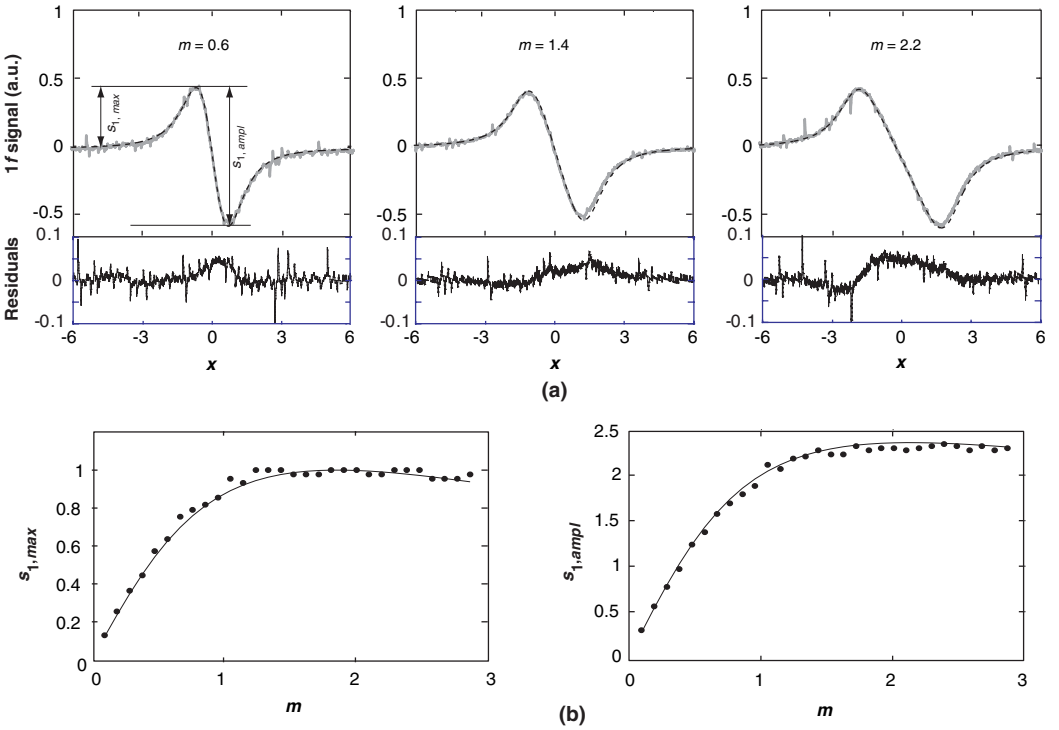

Fig. 6. (a) Normalized WM-PAS $1f$ signal for different values of the modulation index m. Grey lines are experimental measurements and dashed curves have been calculated from our theoretical model. (b) Maximum ($s_{1,\max}$) and amplitude ($s_{1,\mathrm{ampl}}$) of the $1f$ signal as a function of the modulation index m. These two parameters are defined on the $1f$ signal in (a). Circles are experimental measurements and the curve is the result of the theoretical model.

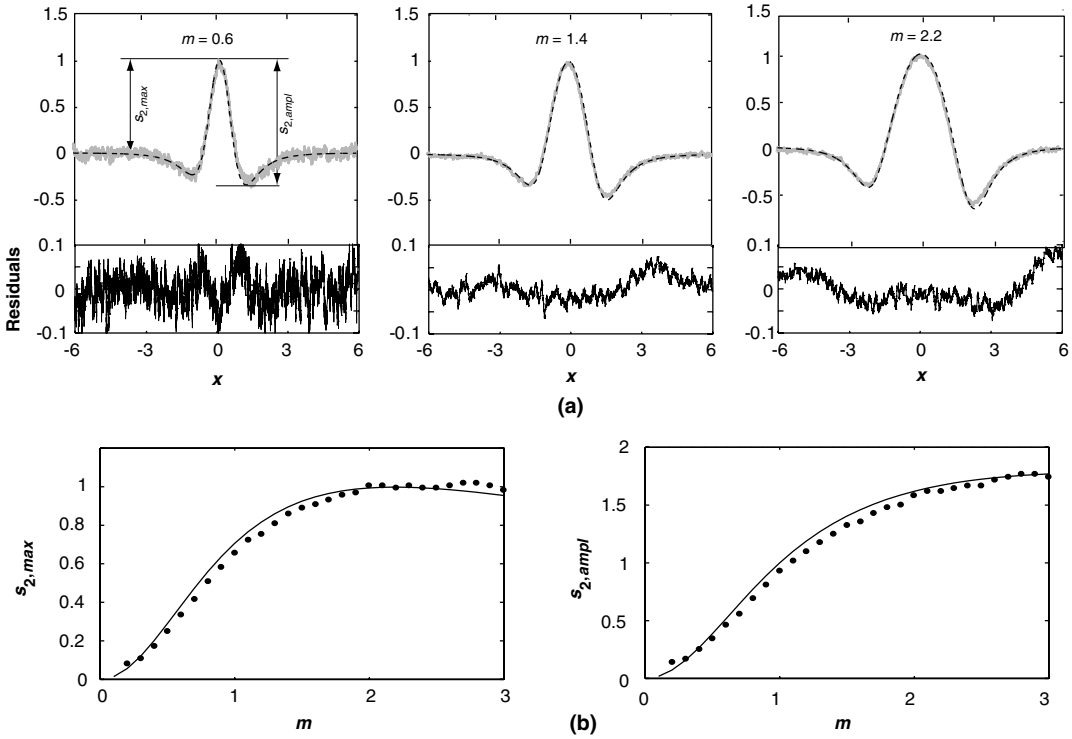

Fig. 7. (a) Normalized WM-PAS 2*f* signal for different values of the modulation index *m*. Grey lines are experimental measurements and dashed curves have been calculated from our theoretical model. (b) Maximum ($s_{2,\max}$) and amplitude ($s_{2,\mathrm{ampl}}$) of the 2*f* signal as a function of the modulation index *m*. These two parameters are defined on the 2*f* signals in (a). Circles are experimental measurements and the curve is the result of the theoretical model.

analysis of WM-PAS signals. The different modulation frequencies experimentally used to measure the two first harmonic PA signals are summarized in Table 2. The corresponding WM-PAS signals are shown in Fig. 5 together with the WMS signals previously obtained using the same laser modulation parameters and a 1-m absorption cell [25]. As expected, these signals are very similar, excepted for the 1*f* component, whose background level is zero for PAS, whereas a quite large offset occurs in the WMS signal due to laser residual amplitude modulation. Influence of FM index *m* on 1*f* and 2*f* WM-PAS signals is shown in Figs. 6 and 7. The comparison of experimental signals with the results of our theoretical model shows good agreement, as indicated by the residuals reported in each case. These results validate the relevance of the developed model. However, the residuals increase for higher values of *m* ($m > 2$), so that the agreement between experimental and theoretical values becomes slightly worse. This is probably due to the non-linear behavior of the laser optical frequency versus injection current that is observed at large modulation depths. For small modulation indices ($m \ll 1$), the harmonic PA signals increase and get broader when increasing *m*. An optimal modulation index is obtained at each harmonic, for which the amplitude of the PA signal reaches its maximum value. For a Lorentzian absorption lineshape, the optimal values are $m \cong 2.00$ and $m \cong 2.20$ for 1*f* and 2*f* signals, respectively, as already demonstrated for WMS [22]. Above these values, the harmonic PA signal continues to broaden, but its amplitude slowly tends to diminish.

4. Discussion and conclusion

Analytical expression of harmonic signals generated by WM-PAS has been proposed in the general case of combined WM-IM of a laser diode. This description is based on a previous model we developed for WMS. This model was modified by taking into account the fundamental difference between these two techniques, i.e. in WMS, the optical energy transmitted through the analyzed sample is detected, whereas the absorbed energy is directly measured in

WM-PAS. This theoretical model has shown that PA signals generated with combined IM–FM are identical, except for the sign, to those obtained by WMS. However, important difference occurs in the first harmonic signal, which usually presents a large offset value in the case of WMS, whereas offset-free signal is obtained by WM-PAS. This property results from the zero-background nature of PAS.

The reported model applies for combined WM-IM with arbitrary phase shift Ψ between the two modulations, which is the real condition when the injection current of a laser diode is modulated. This model considers a Lorentzian absorption line and is therefore suitable for WM-PAS trace-gas detection at atmospheric pressure, for which the Voigt lineshape is well approximated by a Lorentzian function. The harmonic signals calculated from this model have been compared with experimental results obtained by WM-PAS on a CO_2 absorption line using a 2-μm DFB laser. Excellent agreement has been obtained between experimental and calculated signals, which validates the relevance of the developed theoretical model. However, the agreement has shown to be slightly reduced when larger FM indices ($m > 2$) are used, which probably results from the non-linear behavior of the laser optical frequency versus injection current that is experimentally observed at large modulation depths and that is not taken into account in the model, since only linear dependence is considered.

Finally, the description presented in this paper enables better understanding of the signals generated in WM-PAS and gives useful information to define the optimal laser modulation amplitude in WM-PAS trace-gas detection.

References

[1] D.T. Cassidy, J. Reid, Atmospheric pressure monitoring of trace gases using tunable diode lasers, Appl. Opt. 21 (1982) 1185–1190.

[2] G.C. Bjorklund, Frequency-modulation spectroscopy: a new method for measuring weak absorptions and dispersions, Opt. Lett. 5 (1980) 15–17.

[3] H. Lotem, Extension of the spectral coverage range of frequency-modulation spectroscopy by double frequency-modulation, J. Appl. Phys. 54 (1983) 6033–6035.

[4] M.W. Sigrist, Trace gas monitoring by laser photoacoustic spectroscopy and related techniques, Infrared Phys. Technol. 36 (1995) 415–425.

[5] S. Schilt, L. Thévenaz, M. Niklès, L. Emmenegger, C. Hüglin, Ammonia monitoring at trace level using photoacoustic spectroscopy in industrial and environmental applications, Spectrochim. Acta A 60 (2004) 3259–3268.

[6] M.B. Pushkarsky, M.E. Webber, O. Baghdassarian, L.R. Narasimhan, C.K.N. Patel, Laser-based photoacoustic ammonia sensors for industrial applications, Appl. Phys. B 75 (2002) 391–396.

[7] L.B. Kreuzer, in: Y.-H. Pao (Ed.), Optoacoustic Spectroscopy and Detection, Academic Press, New York, 1977, pp. 1–25, Chap. 1.

[8] A. Miklos, P. Hess, Z. Bozoki, Application of acoustic resonators in photoacoustic trace gas analysis and metrology, Rev. Scient. Instr. 72 (2001) 1937–1955.

[9] P.L. Meyer, M.W. Sigrist, Atmospheric pollution monitoring using CO_2-laser photoacoustic spectroscopy and other techniques, Rev. Sci. Instr. 61 (1990) 1779–1806.

[10] M.E. Webber, M. Pushkarsky, C.K.N. Patel, Fiber-amplified-enhanced photoacoustic spectroscopy with near-infrared tunable diode lasers, Appl. Opt. 42 (2003) 2119–2126.

[11] J.-Ph. Besson, S. Schilt, L. Thévenaz, Sub-ppb ammonia detection based on photoacoustic spectroscopy, in: 17th International Conference on Optical Fibre Sensors, Bruges, Belgium, May 23–27, 2005, P1-32.

[12] B. Paldus, T.G. Spence, R.N. Zare, J. Oomens, F.J.M. Harren, D.H. Parker, C. Gmachl, F. Capasso, D.L. Sivco, J.N. Baillargeon, A.L. Hutchinson, A.Y. Cho, Photoacoustic spectroscopy using quantum-cascade lasers, Opt. Lett. 24 (1999) 178–180.

[13] D. Hofstettler, M. Beck, J. Faist, M. Nägele, M.W. Sigrist, Photoacoustic spectroscopy with quantum cascade distributed-feedback lasers, Opt. Lett. 26 (2001) 887–889.

[14] A.A. Kosterev, Y.A. Bakhirkin, F.K. Tittel, Ultrasensitive gas detection by quartz-enhanced photoacoustic spectroscopy in the fundamental molecular absorption bands region, Appl. Phys. B 80 (2005) 133–138.

[15] M. Fehér, Y. Jiang, J.P. Maier, A. Miklòs, Optoacoustic trace-gas monitoring with near-infrared diode lasers, Appl. Opt. 33 (1994) 1655–1658.

[16] S. Schilt, J.-Ph. Besson, L. Thévenaz, Fibre-coupled photoacoustic sensor for sub-ppm methane monitoring, in: J.M. López-Higuera, B. Culshaw (Eds.), Second European Workshop on Optical Fiber Sensors (Santander, Spain, June 9–11 2004), SPIE Volume 5502, Bellingham Washington, 2004, pp. 317–320.

[17] R. Arndt, Analytical line shape for Lorentzian signal broadened by modulation, J. Appl. Phys. 36 (1965) 2522–2524.

[18] J. Reid, D. Labrie, Second-harmonic detection with tunable diode lasers- comparison of experiment and theory, Appl. Phys. B 26 (1981) 203–210.

[19] J.M. Supplee, E.A. Whittaker, W. Lenth, Theoretical description of frequency modulation and wavelength modulation spectroscopy, Appl. Opt. 33 (1994) 6294–6302.

[20] L.C. Philippe, R.K. Hanson, Laser diode wavelength-modulation spectroscopy for simultaneous measurement of temperature, pressure, and velocity in shock-heated oxygen flows, Appl. Opt. 32 (1993) 6090–6103.

[21] P. Kluczynski, O. Axner, Theoretical description based on Fourier analysis of wavelength-modulation spectrometry in terms of analytical and background signals, Appl. Opt. 38 (1999) 5803–5815.

[22] P. Kluczynski, J. Gustafsson, A. Lindberg, O. Axner, Wavelength modulation absorption spectrometry—an extensive scrutiny of the generation of signals, Spectrochim. Acta B 56 (2001) 1277–1354.

[23] P. Kluczynski, A. Lindberg, O. Axner, Background signals in wavelength-modulation spectrometry with frequency-doubled diode-laser light. I. Theory, Appl. Opt. 40 (2001) 783–793.
[24] P. Kluczynski, A. Lindberg, O. Axner, Background signals in wavelength-modulation spectrometry with frequency-doubled diode-laser light. II. Experiment, Appl. Opt. 40 (2001) 794–805.
[25] S. Schilt, L. Thévenaz, P. Robert, Wavelength modulation spectroscopy: combined frequency and intensity laser modulation, Appl. Opt. 42 (2003) 6728–6738.
[26] M. Szakall, Z. Bozóki, A. Mohácsi, A. Varga, G. Szabó, Diode laser based photoacoustic water vapor detection system for atmospheric research, Appl. Spectrosc. 58 (2004) 792–798.
[27] J. Ng, A.H. Kung, A. Miklós, P. Hess, Sensitive wavelength-modulated photoacoustic spectroscopy with a pulsed optical parametric oscillator, Opt. Lett. 29 (2004) 1206–1208.
[28] A. Stark, L. Correia, M. Teichmann, S. Salewski, C. Larsen, V.M. Baev, P.E. Toschek, Intracavity absorption spectroscopy with thulium-doped fibre laser, Opt. Commun. 215 (2003) 113–123.
[29] M. Wolff, H. Harde, Photoacoustic spectrometer based on a DFB-diode laser, Infrared Phys. Technol. 41 (2000) 283–286.
[30] A. Miklòs, Z. Bozóki, Y. Jiang, M. Fehér, Experimental and theoretical investigation of photoacoustic signal generation by wavelength-modulated diode laser, Appl. Phys. B 58 (1994) 483–492.
[31] L.S. Rothman, C.P. Rinsland, A. Goldman, S.T. Massie, D.P. Edwards, J.-M. Flaud, A. Perrin, C. Camy-Peyret, V. Dana, J.Y. Mandin, J. Schroeder, A. McCann, R.R. Gamache, R.B. Wattson, K. Yoshino, K.V. Chance, K.W. Jucks, L.R. Brown, V. Nemtchinov, P. Varanasi, The HITRAN molecular spectroscopic database and HAWKS (HITRAN atmospheric workstation): 1996 edition, J. Quant. Spectrosc. Radiat. Transfer. 60 (1998) 665–710.